Journal of Catalysis 269 (2010) 269–280

Contents lists available at ScienceDirect

Journal of Catalysis

journal homepage: www.elsevier.com/locate/jcat

The influence of reducing and sulfiding conditions on the properties of unsupported MoS_2-based catalysts

Pavel Afanasiev *

Institut de recherches sur la catalyse et l'environnement de Lyon UMR5256, CNRS-Université de Lyon 1, 2 Avenue Albert Einstein, 69626 Villeurbanne Cedex, France

ARTICLE INFO

Article history:
Received 29 October 2009
Revised 3 November 2009
Accepted 3 November 2009

Keywords:
Molybdenum sulfide
Hydrogenation
Hydrodesulphurization
Thiophene
Temperature-programmed reduction
Transmission electron microscopy

ABSTRACT

Unsupported MoS_2 catalysts were obtained from the decomposition of ammonium tetrathiomolybdate (ATM) at variable temperatures (400–700 °C) and under different gas compositions, from pure H_2S to pure H_2. The catalysts were further studied in the non-promoted state or promoted by Ni and Co. Catalytic activity and selectivity were studied in the model reaction of thiophene hydrodesulfurization (HDS). Surface areas, crystalline phase and particle size distributions were determined by Brunauer–Emmet–Teller (BET), X-ray diffraction (XRD) and transmission electron microscopy (TEM), respectively. A comparison of average values calculated from these techniques has enabled the understanding of the morphology of the solids. The catalysts were characterized before and after catalytic tests by X-ray photoelectron spectroscopy (XPS), laser Raman spectroscopy (LRS) and temperature-programmed reduction (TPR).

Comparison of catalytic activity trends with the results of the characterizations show that overstoichiometric sulfur, present in the fresh catalysts in the form of edge-located S_2^{2-} species, plays a key role for the activity of unsupported MoS_2 and for its ability to be promoted. Direct hydrogenation (HYD) of thiophene to butane occurs presumably with the participation of –SH groups, produced from the opening of S–S bridges by hydrogen. Whatever the gas atmosphere, any treatment leading to the removal of overstoichiometric sulfur leads to a decrease in HYD selectivity. Thus, very similar catalytic properties were observed for MoS_2 annealed at 700 °C in pure H_2, H_2S or N_2 gases. Ni and Co introduced by means of reflux with acetylacetonates, gave identical promotion trends for all the MoS_2 samples. The solids treated in pure H_2S could not take up promoter atoms at the edges, whereas for the H_2-reduced samples high promotion levels were achieved. The degree of stacking does not seem to have a significant impact on the thiophene HDS activity and selectivity of the unsupported MoS_2 catalysts.

1. Introduction

Transition metal sulfide (TMS) hydrotreating catalysts, used to produce clean motor fuels, are one of the most important industrial catalytic systems [1–3]. Many studies have dealt with the understanding of the genesis and functioning of the TMS catalysts, and particularly of Ni(Co)–Mo mixed sulfides. The main progress in the comprehension of TMS catalysts has been achieved due to the work by Topsøe and colleagues in which an edge-decorated CoMoS phase model has been suggested [4,5]. Later, the results of scanning tunnelling microscopy (STM) allowed confirming the existence of earlier proposed structures [6,7]. Considerable effort has been directed toward atomistic theory models of the catalytically active TMS phases [8–10]. The MoS_2 edge energies and geometry of species as a function of composition were extensively studied [11]. Current models consider the differences between crystallographically distinct MoS_2 slabs terminations, (namely metal M (1 0 $\bar{1}$ 0) and sulfur S ($\bar{1}$ 0 1 0) edges) as a key point for the understanding of catalytic activity and promotion trends [12]. The nature of the exposed edges is expected to depend on the treatment conditions [13].

Despite considerable progress in the field, several important questions are still unresolved. Thus, since the formulation of the rim-edge model by Daage and Chianelli [14], no clarity has been achieved regarding the relationship between the HYD/HDS selectivity and MoS_2 slabs stacking [15–18]. The number of structurally distinct active centres is also still questionable. One-centre model was proposed by Miller et al. [19] for supported CoMoS systems. However, the DDS and HYD activity do not change in step after incorporating Co into Mo sulfide, suggesting that there are at least two types of centres [20]. One of the most basic still unanswered questions is the exact nature of hydrogen activation by MoS_2 particles. Spectroscopic studies of supported and unsupported sulfides have proven the existence of surface disulfide S_2^{2-} species [21,22] and SH groups [23–25] but not for Mo–H species, which would result from H_2 dissociation on the sulfide edges. Recent papers by Polyakov et al. demonstrate the presence of some

* Fax: +33 04 72 44 53 99.
E-mail address: pavel.afanasiev@ircelyon.univ-lyon1.fr

0021-9517/$ - see front matter © 2009 Elsevier Inc. All rights reserved.
doi:10.1016/j.jcat.2009.11.004

hydrogen-containing species on the surface of unsupported overstoichiometric MoS_{2+x}, able to hydrogenate olefins in the absence of H_2 [26,27]. Farag et al. observed that the HYD reaction on MoS_2 is promoted by H_2S [28]. These findings have no direct interpretation within the framework of existing models.

Low valence sulfur (S_2^{2-}) species located on the MoS_2 edges were supposed earlier to be involved in H_2 activation [29]. In our recent work [30,31] evidence for homolytic low-temperature H_2 dissociation on S–S bridges has been presented for the amorphous sulfides CoSOH and MoS_3. An effect of hydrogen interaction with S_2^{2-} groups on the catalytic performance seems to be a plausible hypothesis. Therefore, the goal of the present work is to contribute to the understanding of key properties of the MoS_2 catalysts by studying well characterized unsupported catalysts with variable stoichiometry. First, the properties of non-promoted MoS_2 are reported, and then promotion with Co and Ni is briefly considered.

2. Experimental

2.1. Catalysts preparation

High-purity ammonium heptamolybdate and ammonium sulfide were purchased from Sigma–Aldrich. Ammonium tetrathiomolybdate, $(NH_4)MoS_4$, (ATM) was obtained by the addition at ambient temperature of 15 g of $(NH_4)_6Mo_7O_{24}{\cdot}4H_2O$ to 200 mL of a 20 wt% solution of $(NH_4)_2S$, upon stirring. The mixture was stirred for several hours, and then kept in a refrigerator for one week. Dark red crystals precipitated, which were filtered, washed with cold ethanol, dried, and stored under nitrogen.

Decomposition of ATM was carried out in Pyrex or quartz reactors. A weighted amount of ca. 2 g ATM was placed in a reactor and treated in a gas flow of 60 mL/min of pure H_2, pure H_2S or 15% vol. H_2S/H_2. The temperature was raised at a rate 5° min^{-1} to a desired value and kept for several hours. During the treatment and the following cooling, the gas composition was kept constant or was varied, and this represents an important point of the experimental procedure. The conditions of preparation are listed in Table 1. Self-explanatory designations of the catalysts are applied whenever possible. For example, the sample sulfided in pure H_2S at 500 °C is named S-500, whereas the solid first sulfided and then treated in pure hydrogen at 400 °C is designated SH-400. A reference MoS_3 amorphous sulfide was obtained by acidification of the ATM aqueous solution, as described in [31].

Promoted catalysts were prepared according to Ref. [32]. In brief, a weighted amount of Ni or Co acetylacetonate complex was dissolved in a minimum amount of methanol while flushed by nitrogen. Then MoS_2 powder was added to the solution in an atomic ratio of Co(Ni)/Mo = 0.4 and then the suspension was heated at the boiling temperature of methanol (65 °C) for 4 h without admission of air. To achieve complete interaction, the mixtures were cooled to room temperature and kept overnight under nitrogen. Afterward, the solids were recovered by filtration and dried under N_2 at room temperature. The catalysts were tested as such or after re-sulfidation with H_2/H_2S at 350 °C for 1 h.

2.2. Characterization and catalytic tests

Temperature-programmed reduction (TPR) was carried out in a quartz reactor. Samples of sulfides (ca. 0.005–0.01 g) were heated under a hydrogen flow (50 cm^3/min) from room temperature to 1050 °C at a rate of 5° min^{-1}. The H_2S evolved in the reduction was detected by means of a HNU photoionization detector equipped with a 10.2 eV UV light source. Other gases were detected by a VG Thermo quadrupole mass-spectrometer. The amount of H_2S released from the solid was quantified after calibration of the detector with a gas mixture of known H_2S content. Temperature-programmed desorption (TPD) was carried out in the same device. The solids were treated in hydrogen at a given temperature, cooled to room temperature and then hydrogen was replaced by a flow of pure argon. After a stabilization period of 0.5–1 h, linear heating was commenced to obtain the TPD traces. The desorbed hydrogen was detected by a mass-spectrometer.

Transmission electron microscopy (TEM) was carried out on a JEOL 2010 device with an accelerating voltage 200 keV. The samples were dispersed in *n*-hexane by ultrasound, and then put onto a holey carbon filament on a copper grid sample holder. In order to protect them from oxidation by air, the samples still covered with liquid hexane were immediately introduced into the vacuum chamber. The analysis of images (slabs stacking and length) was carried out using Digital Micrograph Gatan™ software. The average slab lengths (L) and stacking layer numbers (N) were calculated as the first moments of the respective distributions.

Nitrogen adsorption–desorption isotherms were measured on a Micromeritics ASAP 2010 instrument. Pore size distributions in the mesopores domain were calculated by the Barrett–Joyner–Hallenda (BJH) method. The BJH pore size distributions were calculated from the desorption branch of the isotherms. Prior to measurements the samples were heated in a secondary vacuum at 300 °C for 4 h. The X-ray diffraction (XRD) patterns were obtained on a Bruker diffractometer with Cu Kα emission and identified using standard JCPDS files. Mean particles size was determined using the Scherrer equation. Laser Raman spectra of sulfides were obtained using a LabRam HR spectrometer (Jobin Yvon) equipped with a CCD detector. The exciting line at 514.53 nm of an Ar^+–Kr^+ RM 2018 laser (Spectra Physics) was focused on each point with a 100× objective and a power of ca. 1 mW. To protect them from air, the samples were sealed in Pyrex capillaries under inert atmosphere. X-ray photoelectron spectroscopy (XPS) studies were performed on a VG ESCALAB 200R spectrometer using Al Kα radiation. The XPS spectra of O 1s and S 2p and Mo 3d were recorded and their binding energies (BE) referred to the energy of the C 1s peak (BE 285.0 eV). Quantification of the surface contents of the elements was done using the sensitivity factors provided with the VG software. The metals content in the synthesized solids was determined, after dissolution in a HNO_3/H_2SO_4 mixture, by plasma-coupled atomic emission spectroscopy (AES-ICP). The sulfur and carbon contents were measured with a Strohlein Instruments CS-MAT 5500 analyzer.

Catalytic activities were measured for thiophene HDS at atmospheric pressure in a fixed-bed flow microreactor. In the chosen temperature range, 280–320 °C, the thiophene conversion was below 10% under the conditions used (50 mL/min gas flow, 50–500 mg of catalyst), and the plug-flow reactor model was used to calculate the specific reaction rate, V_s, according to equation

$$V_s = -(F/m)\ln(1-x)$$

where F is the thiophene molar flow (mol/s), m is the catalyst mass (g), and x is the thiophene conversion. To compare the catalysts evolution on a common basis, HDS activity at 300 °C was measured every 1 h for 80 h at different thiophene molar feed rates (3.0 and 1.0 h^{-1}) and at two levels of thiophene partial pressure (2.85 and 0.64 kPa).

3. Results and discussion

3.1. Non-promoted MoS_2 catalysts

3.1.1. Properties of MoS_2 solids as a function of treatment conditions

To study MoS_2 catalytic properties as a function of stoichiometry and morphology, simple model systems with a minimal num-

Table 1
Preparation conditions and properties of unsupported catalysts studied in this work.

Sample name	Preparation conditions	A_{thio}[a]	$C_4^0/C_4^=$[b]	TEM L/S[c]	D_{XRD}^{002} (nm)[d]	Ssp (m^2/g)[e]	Chemical composition[f]
Non-promoted catalysts							
SH-400	H_2/H_2S 400° 2 h, H_2 400° 4 h	12	0.23	6.1/4.7 6.7/5.1	3.6/3.6	66/17	$H_{0.036}MoS_{2.03}/H_xMoS_{2.05}$
SS-400	H_2/H_2S 400° 2 h, H_2S 400° 4 h	24	0.95	5.5/4.5 5.6/4.3	3.0/3.1	71/16	$MoS_{2.26}/H_xMoS_{2.09}$
H-400	H_2 400° 2 h	14	0.27	6.0/4.1	3.6/.37	88/18	$H_{0.042}MoS_{2.04}$
S-400	H_2S 400° 4 h	23	0.78	5.0/4.5	3.8/3.9	82/16	$MoS_{2.28}/H_xMoS_{2.11}$
S-400-H-200	H_2/H_2S 400° 2 h, H_2 200° 4 h	13	0.33	5.5/4.4 5.8/4.8	3.4/2.9	59/13	$H_{0.073}MoS_{2.07}$
SH-500	H_2/H_2S 500° 2 h, H_2 500° 4 h	6	0.13	16/7.0 16/7.2	5.2/5.5	16/7	$H_{0.006}MoS_{1.93}/H_xMoS_{1.98}$
SS-500	H_2/H_2S 500° 2 h, H_2S 500° 4 h	9	0.25	15/7.5 16/7.4	5.2/4.8	17/8	$MoS_{2.04}/HxMoS_{2.01}$
H-500	H_2 500° 2 h	10	0.09	14/7.2	5.0/5.4	18/7	$H_{0.008}MoS_{1.95}$
S-500	H_2S 500° 2 h	11	0.24	–	4.8/4.6	21/8	$MoS_{2.06}$
SH-700	H_2/H_2S 700° 2 h, H_2 700° 4 h	2.5	0.07	–	11.0/10.5	5/5	$H_{0.002}MoS_{1.86}/HxMoS_{1.93}$
SS-700	H_2/H_2S 700° 2 h, H_2S 700° 4 h	3	0.08	23/9.5 22/10	9.7/9.9	6/4	$MoS_{2.00}$
S-700	700° 1 h; H_2S	4	0.09	–	9.5/9.5	5/4	$MoS_{2.01}$
SN-700	H_2/H_2S 700° 2 h, H_2S 700° 4 h	4	0.06	–	9.8/9.8	5/3	$MoS_{2.00}$
MoS_3	Aqueous precipitation	50	0.98	–	–/3.5	–/26	$MoS_{3.04}/H_xMoS_{2.17}$
Promoted catalysts							
Ni–SH-400		52	0.16	5.8/5.0	3.6/3.7	56/13	$Ni_{0.058}MoS_{2.04}$
Co–SH-400		50	0.13	–	3.5/3.5	61/13	$Co_{0.043}MoS_{2.06}$
Ni–SS-400		25	0.49	–	3.2/3.0	70/15	$Ni_{0.018}MoS_{2.25}$
Co–SS-400		22	0.55	5.1/4.8	3.6/3.4	67/12	$Co_{0.016}MoS_{2.25}$
Ni–S-400-H-200		51	0.18	–	3.0/3.4	62/11	$Ni_{0.078}MoS_{2.08}$
Co–S-400-H-200		53	0.20	5.7/4.8	3.3/3.3	58/11	$Co_{0.048}MoS_{2.09}$
Ni–H-400		84	0.18	–	3.5/4.0	77/14	$Ni_{0.074}MoS_{2.06}$
Ni–S-400		17	0.64	–	3.3/3.6	70/16	$Ni_{0.019}MoS_{2.26}$
Co–SS-500		10	0.17	–	5.4/5.2	19/8	$Co_{0.010}MoS_{2.03}$
Co–SH-500		9	0.09	–	5.8/5.8	18/7	$Co_{0.012}MoS_{1.97}$
Ni–SS-700		4	0.1	–	9.7/9.7	7/4	$Ni_{0.004}MoS_{2.00}$
Co–MoS_3		35	0.75	–	–/3.3	–/28	$Co_{0.015}MoS_{2.12}$

[a] Stationary thiophene conversion rate at 300 °C, 10^{-8} mol g^{-1} s^{-1}.
[b] Ratio of butane production rate to the sum of butenes, at 3% total conversion and 300 °C.
[c] L is average length, nm, S is average slabs stacking, as determined from TEM; second line (if present) is for the sample after catalytic test.
[d] XRD-derived slabs stacking before/after catalytic test.
[e] BET specific surface area before/after catalytic test.
[f] Chemical composition before/after catalytic test (if only one number is given it corresponds to the value before test).

ber of unknown parameters are preferable. Unsupported MoS_2 catalysts obtained from ATM decomposition were chosen as such model systems. The conditions of decomposition were adjusted to favour formation of sulfur-saturated or reduced S- and M-edges and/or to produce different amounts of the S_2^{2-} surface groups.

Thiomolybdates have been widely used as sources for MoS_2-based catalysts [33–35]. ATM decomposition in an inert atmosphere and under H_2 was studied in [36,37]. The reaction is complete at 400 °C and occurs according to the two-step sequence [(1) and (2)].

$$(NH_4)_2MoS_4 = MoS_3 + 2NH_3 + H_2S \quad (1)$$

$$MoS_3 = MoS_2 + 1/4S_8 \quad (2)$$

Hydrogen can assist ATM decomposition, removing some part of the sulfur in the form of H_2S. While Eqs. (1) and (2) describe formation of the stoichiometric sulfide, the exact composition of the product depends on the treatment atmosphere. Treatment by H_2S leads to atomic ratios S/Mo > 2, whereas heating in H_2 yields solids with S/Mo < 2 ratios.

Treatment under different conditions yielded solids with variable crystallinity and stoichiometry. The results of characterizations are listed in Table 1. Only the MoS_2 phase was observed in all the solids by powder X-ray diffraction. Analysis of the XRD patterns showed the expected narrowing of the XRD lines with increase of treatment temperature (Fig. 1 and Table 1). Narrowing of the XRD peaks was accompanied with a decrease in the specific surface areas and an increase of the length and stacking of the MoS_2 slabs. The latter effect was confirmed by statistical analysis of the slabs in the TEM images (Figs. 2 and 3). The MoS_2 slabs in the solids treated at 400 °C were often bent, but with the increase of temperature the stacks became more straight (Fig. 2). No difference between the morphology of H_2S-treated and H_2-treated samples could be noted visually. The estimates of stacking derived from the XRD and TEM measurements are coherent and showed both a slightly greater stacking for the H_2-treated samples as compared to those heated in pure H_2S. Due to agglomeration of the stacks in bundles, the observed BET surface areas are much lower than could be inferred from the length and stacking of the layers (calculated values are about 250 m^2/g for the samples treated at 400 °C). Such discrepancies were observed earlier for the ATM-derived MoS_2 catalysts [38,39]. Overall, the effect of gas atmosphere on the morphological properties of unsupported MoS_2 is much smaller than that of temperature.

According to the chemical analysis data, atomic ratios of S/Mo > 2 were found for all the samples treated in H_2S, but also in the samples reduced by H_2 at 400 °C, which remained slightly over-stoichiometric despite the reductive conditions. The amount of extra sulfur in the solids decreased with increase of the treatment temperature, whatever the gas used. The removal of sulfur occurred apparently due to two reasons. First, the over-stoichiometric sulfur species seemed to be unstable above 400 °C even in the

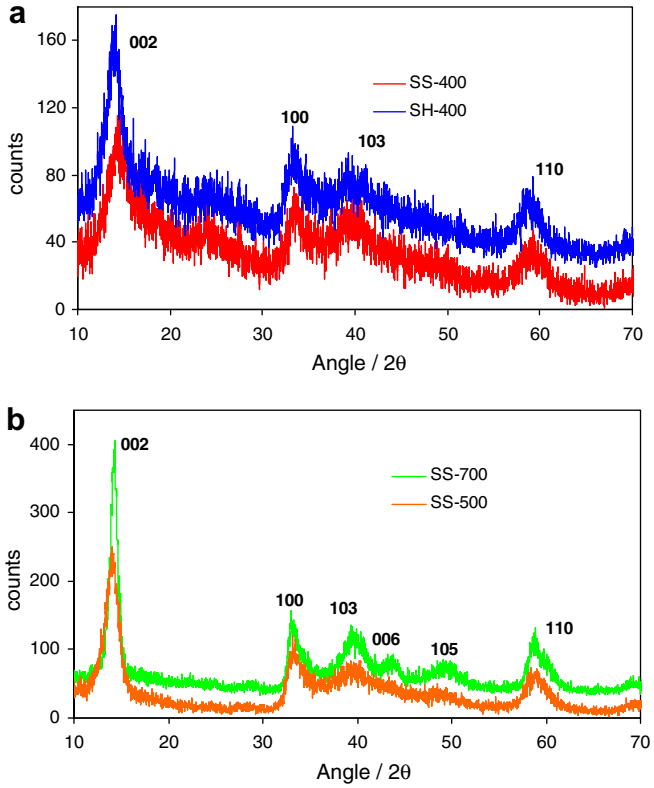

Fig. 1. XRD patterns of unsupported MoS_2 catalysts: (a) treated at 400 °C; (b) treated at 500 °C and 700 °C. Miller indexes of the crystallographic planes are indicated near the corresponding peaks.

H_2S flow. Second, thermal sintering of MoS_2 occurred whatever the gas atmosphere, leading to increase of the slabs length and by consequence to decrease of the relative amount of the edge planes capable of bearing extra sulfur.

The nature of over-stoichiometric sulfur in MoS_2 is yet unclear and sometimes referred to as unspecified "weakly bonded sulfur" species [40]. This term may imply a multitude of species including adsorbed H_2S or elemental sulfur. Such possibilities should be ruled out. The presence of H_2S adsorbed on the SS-400 was excluded since prior to the TPR experiments, the solids were pre-heated at 250 °C in a nitrogen flow, and they gave virtually the same TPR curves as without such pre-heating. Then to check whether the elemental sulfur is present in the solids, weighted amounts of freshly prepared samples (ca. 500 mg) were extracted for 1 h under vigorous stirring with 5 mL of chemically pure CS_2 (dry residual in the solvent being less than 0.01%). Then CS_2 was evaporated under a nitrogen flow on a warm heating plate. No solid residue at all could be collected after evaporation of the CS_2. Therefore, the presence of free sulfur in the solids can be safely ruled out. The over-stoichiometric sulfur is therefore bonded to the surface of MoS_2 catalysts. A similar conclusion that the sulfur species responsible for the low-temperature TPR peak is easily reducible but firmly bonded to MoS_2, was obtained in [41].

Temperature-programmed desorption (TPD) was applied to follow the evolution of the amount and nature of hydrogen reversibly adsorbed on the solids. Selected TPD patterns are shown in Fig. 4. The amount of H_2 desorbed by MoS_2 decreased rapidly with increase of the reduction temperature. At the same time, the position of the desorption maxima drifted towards higher temperatures. Hydrogen uptake was always lower by orders of magnitude than could be accommodated by BET surface area, but corresponded to a fraction of 10–30% of the edge-located Mo atoms. As far as comparison is possible, our TPD results are in a good agreement with earlier work on the properties of unsupported MoS_2 as a function of reduction treatment. The literature values of hydrogen uptake by MoS_2 demonstrate considerable scattering caused by different measurement conditions and determination methods. The values found in the present work are in semi-quantitative agreement with the experiments by Komatsu and Hall [42] and Polyakov et al. [26], but are considerably greater than determined by Jalowiecki et al. [43] and Li et al. [44]. Our values are close to those found by Polz et al. [22], who studied the volumetric H_2 uptake on polycrystalline MoS_2 (39 m^2/g^{-1}) in the temperature range 423–573 K. It was already supposed in [22] that one of the possible mechanisms of H_2 activation is homolytic dissociation on the disulfide edge groups. An in-depth study of H_2 activation is out of scope of this paper (for an overview of this problem see the review [45]). Our recent work [30,31] provided straightforward evidence that S–S bonds in the molybdenum sulfides can be homolytically opened by hydrogen even at low-temperature.

The most important conclusions of the present work can be made by comparing the solids heated in H_2 to those treated in H_2S, particularly for the SH-400 and SS-400 samples. These latter two solids were therefore characterized in more detail. Both samples were prepared by treatment of ATM in a H_2/H_2S flow at 400 °C, but then one was kept for an additional 4 h and cooled in pure H_2S (SS-400), whereas the other one was kept for 4 h and then cooled in pure hydrogen (SH-400). According to the existing models, the SS-400 solid should contain edges covered by sulfur, whereas the SH-400 should have uncovered S- and Mo-edges [9,13]. Note that this difference is expected to be even stronger for treatment temperatures higher than 400 °C, as follows from the calculations by Raybaud et al. [13].

The catalysts SH-400 and SS-400 showed very different TPR patterns (Fig. 5). A great amount of easily reducible sulfur was present in SS-400 while this sulfur was expectedly suppressed in the SH-400 sample. In the Raman spectra of SS-400, a feature at 528 cm^{-1} was present, which disappeared from the spectrum of the H_2-treated solid SH-400 (Fig. 6). This difference seems to be due to the S_2^{2-} groups at the surface of the S-saturated solid. As we have recently shown, S_2^{2-} groups contained in the amorphous Co and Mo sulfides can activate hydrogen even at room temperature [31]. In agreement with the experiments, DFT calculations by Sun et al. predict that sulfur dimers should be stable at the sulfur-covered M-edges and homolytic hydrogen adsorption on them with formation of SH groups should be an exothermic process [46]. Earlier, S–S bond vibrations at 520–530 cm^{-1} were observed in the amorphous MoS_3 [47] and MoS_2-based catalysts [21,48]. The whole Raman spectra of both solids (not shown) were dominated by lines at 383 and 408 cm^{-1} corresponding to the E^1_{2g}, and A^1_g modes of hexagonal MoS_2, respectively [49].

Additional support for the presence of S_2^{2-} species in the S-saturated sample was provided by the S 2p XPS spectra (Fig. 7). H_2-treated solid SH-400 showed narrower bands composed of a doublet of S $2p_{3/2}$ at 161.9 eV and S $2p_{1/2}$ at 163.1 eV. This doublet is characteristic of S^{2-} species in regular basal plane positions [50]. The SS-400 sample demonstrated a broadening of the signal due to a higher energy shoulder at BE 163.3 eV, attributable to the S_2^{2-} species [51]. Similar higher BE components were major features in the amorphous MoS_3 sulfide (Fig. 7). A chain-like structure of MoS_3 is supposed to contain very abundant S_2^{2-} species [52]. The Mo 3d spectra (not shown) were less diagnostic since the BE of molybdenum seems to be less affected by the nature of the attached sulfur ligands.

Nitrogen adsorption–desorption isotherms of the SS-400 and SH-400 solids are presented in Fig. 8. Both solids give very similar hysteresis loops close to the H4 type, characteristic of slit-like mesopores typical for layered structures [53]. However, macropores

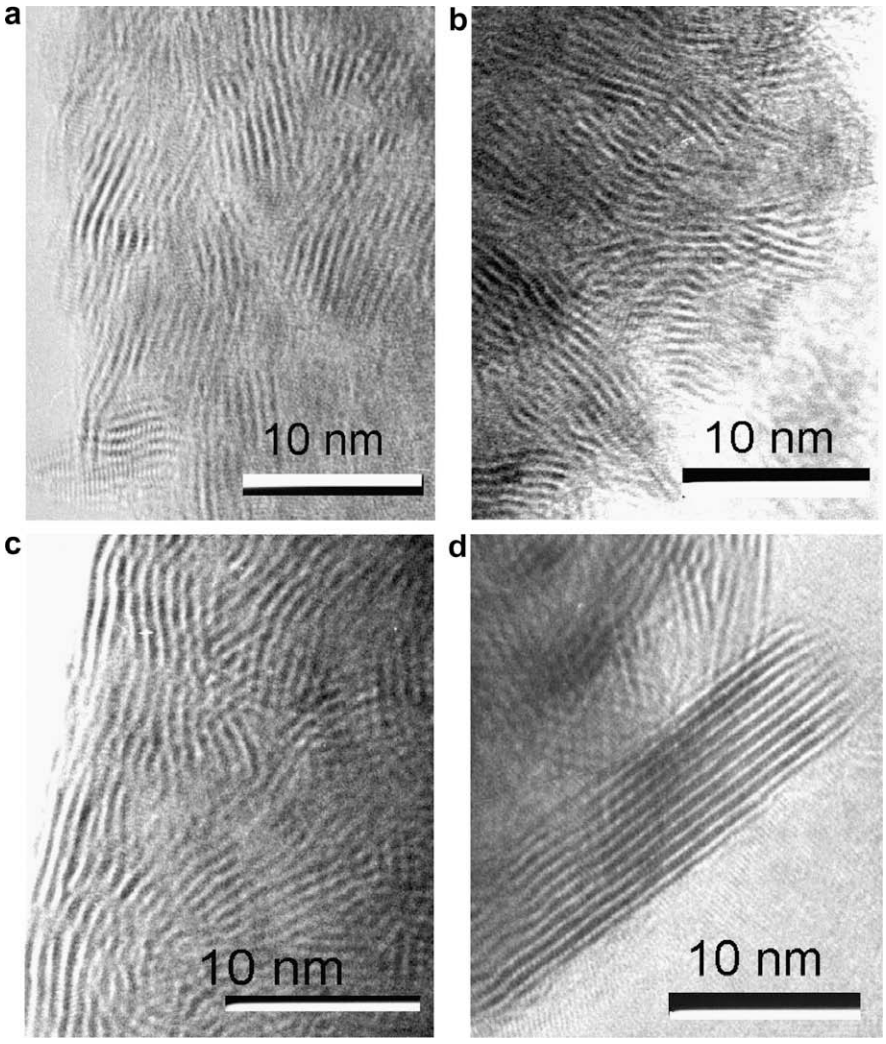

Fig. 2. TEM images of the unsupported MoS_2 catalysts: SS-400 (a), SH-400 (b), SS-500 (c) and SS-700 (d).

and micropores are also present in both samples in non-negligible amounts. Overall, as follows from the comparative characterizations, SS-400 and SH-400 samples have very close morphological characteristics, but differ in chemical composition, due to the presence of abundant over-stoichiometric S_2^{2-} groups in the former and its absence in the latter.

Several other samples were prepared at 400 °C to check the generality of the conclusions and to study the influence of treatment duration on the properties of solids. The solids S-400 and H-400 were prepared by means of less prolonged heating in pure gases. These samples reproduce all the differences between the SS-400 and SH-400 samples but have somewhat higher specific surface areas (Table 1). The sample S-400-H-200 was obtained by heating the pre-sulfided solid in H_2 at 200 °C, the temperature just necessary to remove the sulfur of the first TPR peak. This solid showed morphological characteristics quite similar to those of SH-400 and SS-400 (Table 1).

For the higher temperature preparations SS-500 and SS-700 the TPR patterns showed a drastic decrease of the intensity of the low-temperature peak (Fig. 5b). This seems to be consistent with the decrease in the amount of over-stoichiometric sulfur in these solids. At the same time, due to thermal sintering, the second TPD peak, usually attributed to the reduction of the MoS_2 edges, also decreases. Progressive decrease of this peak with the preparation temperature can be seen from comparison of the low-temperature parts of the curves of SS-500 and SS-700 with that of a solid treated at 400 °C (H-400, Fig. 5b, inset).

3.1.2. Thiophene HDS activity

The thiophene HDS reaction is believed to occur according to a stepwise mechanism including partially hydrogenated intermediates, as presented in Scheme 1. This mechanism is a simplified version of a more detailed scheme, adopted from [54]. Usually, pseudo first-order reaction kinetics equations are used to describe the reaction rate of HDS reaction in a plug-flow reactor [29]. A pseudo first-order HDS reaction kinetics analysis of the relationship between the conversion and the rate constant showed that the standard deviation of the estimated reaction rate constant was less than ±5% in all cases.

Within the series of catalysts prepared at variable temperature, a general trend of decrease of the HDS activity with an increase of the preparation temperature was observed, probably related to thermal sintering. Moreover, after the catalytic test a considerable decrease of the specific surface area was observed for most samples. The evolution of N_2 adsorption–desorption isotherms suggest that this surface area drop is caused by plugging of micropores, since the hysteresis loop was particularly affected at low pressures and in the range of P/P_0 between 0.4 and 0.7 (Fig. 8). The total HDS activity per unit of surface area also decreased with the increase of treatment temperature due to the growth of slabs length and to the

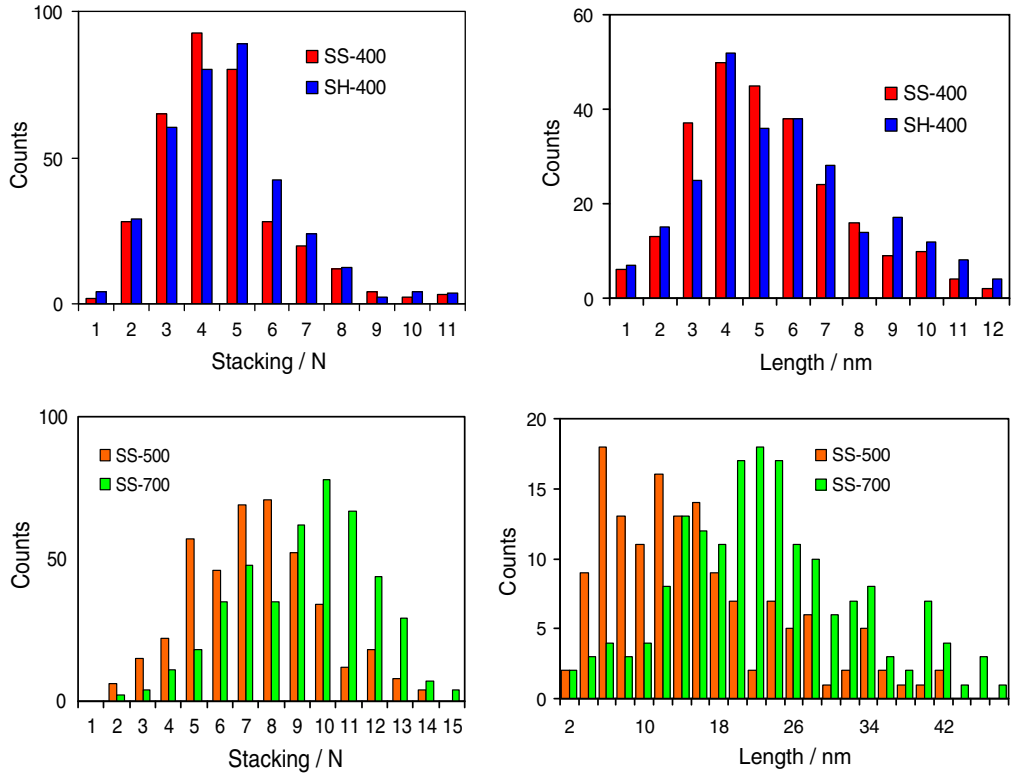

Fig. 3. Distribution histograms of the MoS_2 slabs length and stacking for the samples SS-400, SH-400, SS-500 and SS-700.

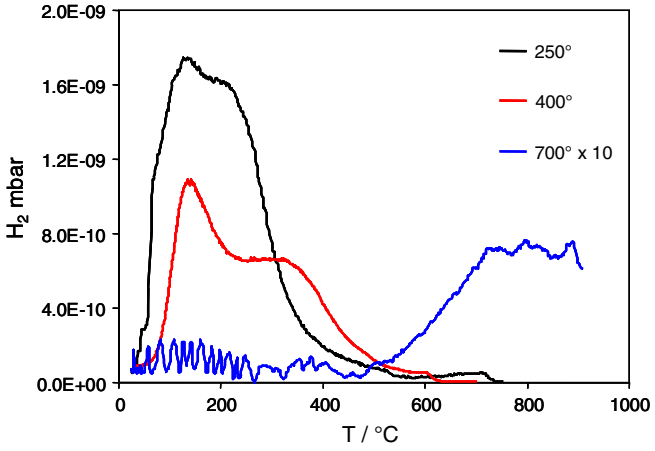

Fig. 4. TPD of hydrogen from the MoS_2 samples treated in H_2 flow at different temperatures.

concomitant decrease of the relative part of the edges in the total surface area. The samples treated in H_2S showed systematically higher activity than H_2-treated ones. This difference was, however, unequal as a function of the preparation temperature. For the solids prepared at 400 °C the difference of the steady state HDS rate was twofold, while it was much lesser for those prepared at 500 °C and almost levelled off for the solids prepared at 700 °C.

In all the experiments, butane/butanes ratio was measured as a function of conversion. We observed that between 0.5% and 5% total conversion, the butane/butenes ratio changed only slightly. At low conversions the butane/butenes ratio was almost a constant with a value depending on the solid preparation. Therefore, we can use the butane/butanes ratio to estimate the HYD/DDS selectivity. This ratio (measured under stationary conditions, at 3–4% conversion) was systematically higher for the samples heated in H_2S than for those treated in H_2 (Table 1). Again, the difference of HYD/DDS selectivity was very high (fourfold) between the solids obtained at 400 °C, it was much lower for those treated at 500 °C and almost inexistent for the solids obtained at 700 °C, whatever the gas atmosphere applied. At the same time the HYD selectivity decreased with increase of treatment temperature, whatever the applied gas.

Such trends of HDS activity cannot be explained by observed morphology variations, since morphology differences between the corresponding H_2S- and H_2-treated solids were only slight. Therefore, the activity and selectivity differences are due to some variation of the chemical state of the solids caused by different gas treatments. The difference is large for the samples prepared at 400°, is smaller at 500° and almost negligible at 700°. The property which changes in exactly the same manner is the solids stoichiometry. An obvious correlation exists therefore between the HDS activity and HYD selectivity and the amount of over stoichiometric sulfur in the solids under study. The higher the amount of extra sulfur, the higher the HDS activity and the higher the HYD selectivity. Note that one of the most active and hydrogenating catalysts was the amorphous MoS_3 reference solid (or rather, the product of its evolution in the reaction mixture at 300 °C, Table 1).

The evolution of activity and selectivity of selected catalysts during the first 24 h of reaction is represented in Figs. 9 and 10. An additional support can be obtained from these results for the relationship between the HYD performance and the amount of over-stoichiometric sulfur. The SS-400 catalyst showed a relatively long stabilization period. The initial activity was very high and after the first 24 h on stream decreased by a factor of six. The HYD selectivity first increased (probably due to the initial opening of S–S bridges, generating SH groups), then decreased (due to the gradual removal of extra sulfur). The results of chemical analysis showed that after the reaction the SS-400 sample lost about 10%

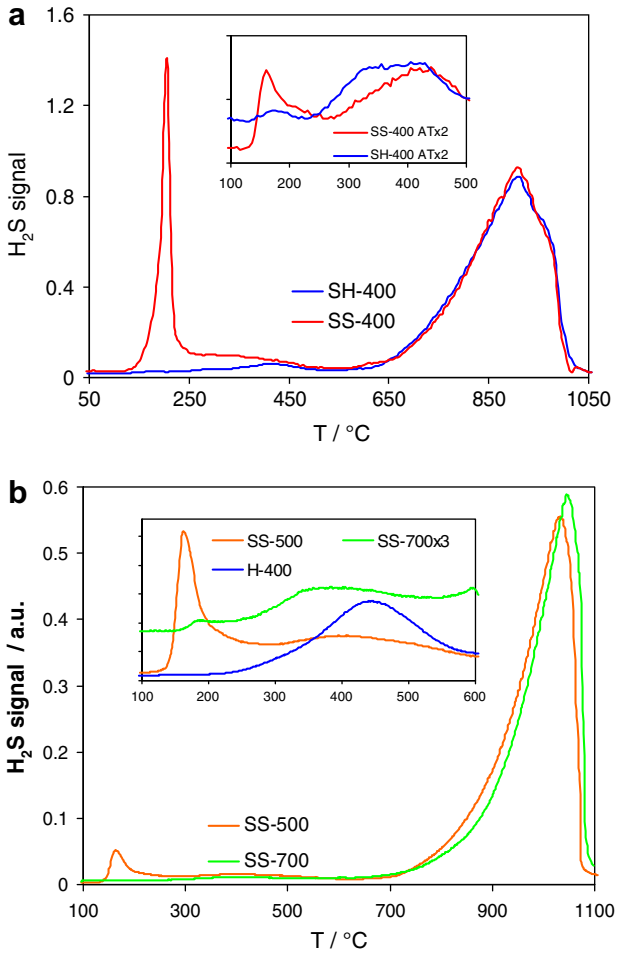

Fig. 5. (a) TPR patterns of MoS_2 samples treated under H_2S and under H_2 at 400 °C. Inset – normalized fragments of TPR curves of the corresponding catalysts after thiophene HDS test; (b) TPR patterns of the solids treated at 500° and 700 °C in pure H_2S. Inset – zoom on the low-temperature parts of the same catalysts and of the H-400 sample, given for comparison.

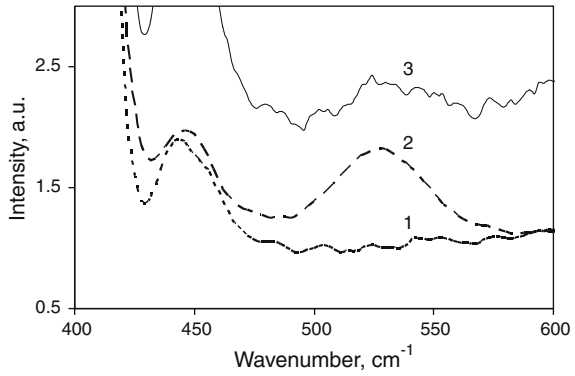

Fig. 6. Laser Raman spectra of the samples SH-400 (1) SS-400 (2) and SS-400 after thiophene HDS test (3).

of its sulfur. By contrast, the transient period for the SH-400 was much shorter. The decrease of SH-400 total HDS activity was only twofold and variations of HYD selectivity were very slight. After the reaction, the SH-400 sample gained a small amount of extra sulfur.

To follow the morphology evolution during the catalytic test, specific surface areas were measured for the solids SS-400 and

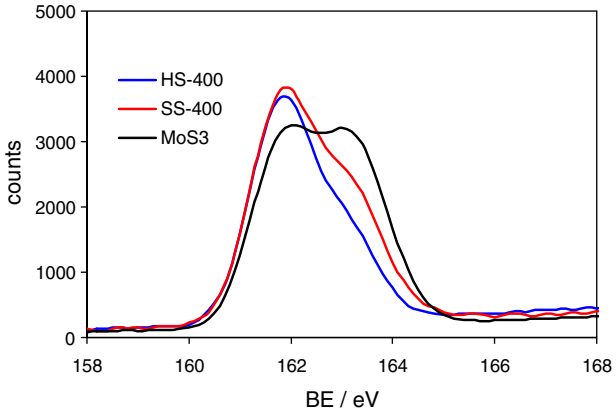

Fig. 7. S 2p XPS spectra of MoS_2, treated at 400 °C under H_2, under H_2S and reference spectrum of the amorphous MoS_3 sulfide. High energy shoulder corresponds to the S_2^{2-} species.

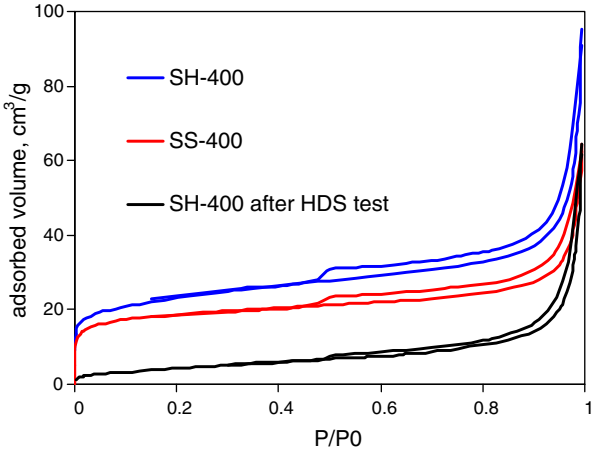

Fig. 8. Low-temperature nitrogen adsorption–desorption isotherms for the samples SS-400, SH-400 and of SH-400 after catalytic test.

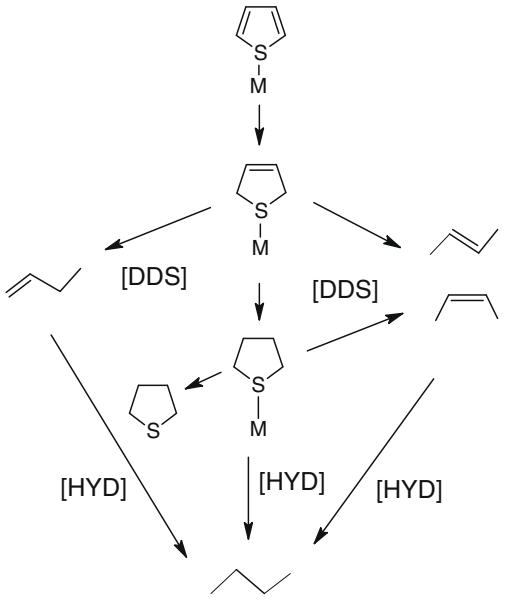

Scheme 1. Thiophene HDS pathways.

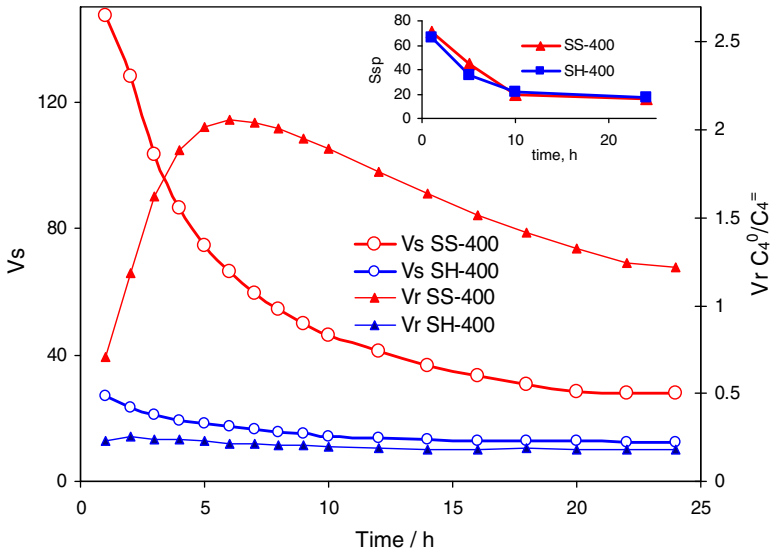

Fig. 9. Time evolution of thiophene conversion rates for the samples SS-400 and SH-400. Left scale – total HDS rate (V_s), 10^{-8} mol g^{-1} s^{-1}; right scale – relative HYD rate (V_r), expressed as ratio of butane production to the sum of butenes. Inset – evolution of the specific surface areas during the test.

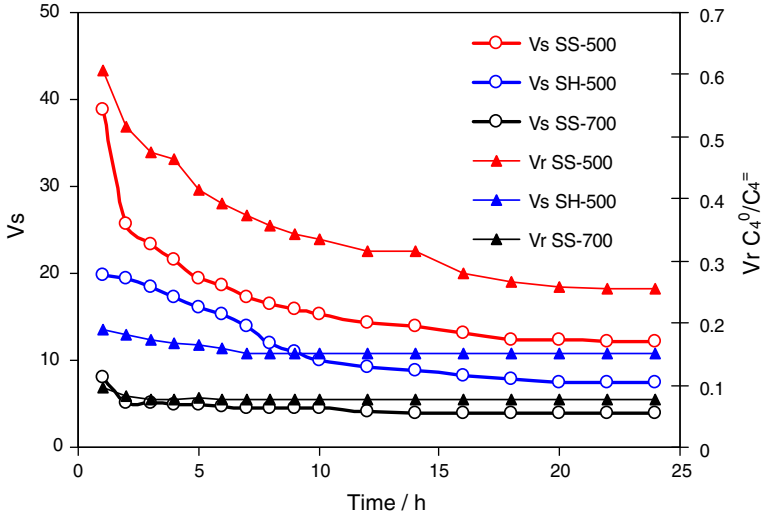

Fig. 10. Time evolution of thiophene conversion rates for the samples SS-500, SH-500 and SS-700. Left scale – total HDS rate (V_s), 10^{-8} mol g^{-1} s^{-1}; right scale – relative HYD rate (V_r), expressed as ratio of butane production to the sum of butenes.

SH-400 arrested after certain time spent in the catalytic reaction. Their surface areas changed nearly perfectly in step (Fig. 9, inset). Therefore, not only initial and final surface areas of the samples were close but their evolution as well was similar. The specific surface area of the SS-400 sample decreased from 71 to 16 m^2/g and at the same time its mass HDS activity dropped from 160 to 24×10^{-8} mol g^{-1} s^{-1}. The surface area of SH-400 decreased from 66 to 17 m^2/g and its mass HDS activity decreased from 22 to 12×10^{-8} mol g^{-1} s^{-1}. Comparison of these numbers shows that specific activity per unit of surface of SS-400 decreased during the transient period, whereas SH-400 even gained some activity. During the same transient period SS-400 lost over-stoichiometric sulfur whereas SH-400 acquired some. However, the difference in sulfur content between these two catalysts remained considerable even after several days of catalytic test. Such a finding might be in seeming contradiction to the existence of a dynamic equilibrium between the MoS_2 surface and the gas phase. Higher conversion of thiophene on the SS-400 catalyst can be rationalized by maintaining a higher H_2S partial pressure over it which allows it to preserve some part of the S_2^{2-} groups. The TPR measurements carried after the thiophene HDS test demonstrated that the amount of sulfur lost by SS-400 and that gained by SH-400 correspond to the variations of the intensity of the first low-temperature peak (Fig. 5a, inset).

Removal of over-stoichiometric sulfur during the HDS test leads to a significant modification of the vibrational and photoelectron spectra. The Raman spectrum of the sample SS-400 measured after HDS test showed the presence of some residual S_2^{2-} groups, but their amount was at the limit of detection (Fig. 6). No evidence of the S–S vibrations was obtained for the tested SH-400 sample. The XPS spectra of the tested samples confirm the decrease of sulfur content in SS-400 and its weak change in SH-400. There is also a strong increase of carbon content in the catalysts after HDS (Table 2). Beside the SS-400 solid, no reliable estimation of

Table 2
XPS contents of the elements on the surface of fresh and tested catalysts.

Sample	S	Mo	S/Mo	C	O	[a]S_2^{2-} (%)
SS-400	53.2	24.4	2.18	17.6	4.9	>7
SS-400 after test	42.0	20.3	2.07	32.3	5.5	<3
SH-400	52.8	26.6	2.02	16.5	4.1	<3
SH-400 after test	42.2	20.8	2.03	30.7	6.1	<3

[a] Percent of total sulfur, estimate.

the S_2^{2-} contribution in other samples was possible using XPS. Neither could we observe any spectroscopic signs of S_2^{2-} species in the high-temperature preparations, before or after catalysis.

Stability experiments for 80 h were carried out at constant temperature (300 °C) to gain a better qualitative understanding of the activity and selectivity evolution during the transient period. Beside the standard HDS conditions described in the experimental part, two types of conditions were applied in these long-duration tests. In the first case (low-flow) the reaction mixture flow rate was decreased threefold, and therefore the contact time was increased correspondingly, leading to a higher instant concentration of H_2S. In the second type of experiment (H_2-diluted), the standard reaction mixture was diluted by a fourfold amount of hydrogen.

We do not analyse here the variations of the overall reaction rate, because a detailed kinetic study is beyond the scope of this work (and rigorous treatment of the problem would be very difficult, since the transient period is under consideration). Worth noting in brief is that in all earlier studies of thiophene HDS kinetics, inhibition by the reaction products and/or lower reaction order by thiophene than by hydrogen were observed [55,56]. As expected, the apparent pseudo first-order constant was strongly increased for the hydrogen-diluted reaction mixture, whereas for the low-flow experiments the reaction rate was much lower than in the standard case. Less affected by the reactants and more relevant to the state of the catalyst surface was the evolution of the product selectivity, as follows.

The curves of time evolution of the butane to butenes ratio are represented in Fig. 11. It can be seen, that for the S-saturated solid, significant modifications of the transient curves were observed, but the variations of the steady state HYD/DDS ratio were only slight. The sharpest and the highest maximum of the HYD/DDS selectivity was observed for the hydrogen-diluted mixture, but the butane to butanes ratio dropped down more rapidly and after 80 on stream was stabilized at the lowest value of 0.68 (Fig. 11, curve 3). By contrast, in the low-flow test (Fig. 11, curve 1) butane selectivity showed the lowest transient peak but its relative decrease was the slowest and it was stabilized at a slightly but significantly higher value of 0.76 (for the standard conditions the corresponding value was 0.72, Fig. 11 curve 2). These findings corroborate the hypothesis that interaction of S_2^{2-} groups with hydrogen produces HYD active sites. Indeed, if the kinetics of S_2^{2-} interaction with hydrogen is affected by the reaction conditions then it should be accelerated by the reactants (H_2) and retarded by the products (H_2S), which is observed in the experiment. On the other hand the equilibrium amount of –SH groups should decrease at higher hydrogen to thiophene ratios, which is again the case.

As with the H-saturated samples, the HYD/DDS ratio changed only weakly throughout the time of the experiment (Fig. 11, curves 4–6). The variations of the reaction mixture composition and time of contact did not lead to any significant changes of butane to butenes ratio. Here, we suppose that the absence of the initial S_2^{2-} groups leads to the absence of HYD/DDS selectivity evolution.

As concerns the solids SS-500 and SH-500, treated at 500 °C, the difference of activity and selectivity between them during the transient period was similar to that between the SS-400 and SH-400 ones, but quantitatively this difference was much smaller (Fig. 10). Finally for the samples treated at 700 °C the HDS activity was virtually stabilized already after 6 h of reaction, and the difference between the H_2 and H_2S-treated samples levelled off. For both solids treated at 700 °C, the butane/butanes ratio was very low. Therefore, it seems to be not the sulfiding/reducing gas atmosphere, but the fact itself of the removal of extra sulfur which leads to the drop of HDS activity and HYD selectivity at higher temperatures. To confirm it, thermal treatment under a non-reacting N_2 atmosphere was carried out (N-700 solid) and the catalytic properties appeared to be close to those of other solids obtained at 700 °C.

The stacking of MoS_2 slabs in the SS-400 and SH-400 samples was almost the same, but their HYD/DDS selectivity was very different. Oppositely, the solids SH-400 and SS-500 showed strongly different stacking values, but close values of HYD/DDS selectivity. This indicates that MoS_2 layers stacking makes probably no direct

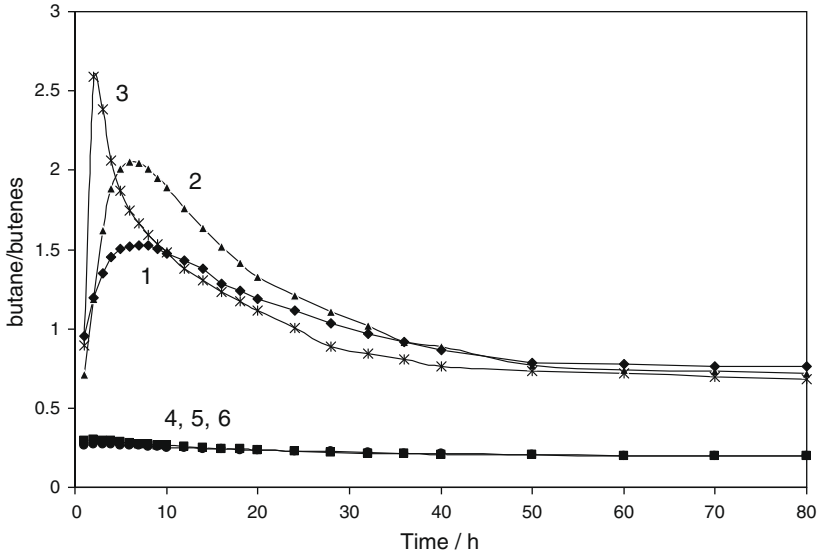

Fig. 11. Stabilization of HYD/DDS activity ratio for SS-400 and SH-400 catalysts tested under different conditions. The curves 1–3 represent SS-400 catalyst; the curves 4–6 correspond to the SH-400 catalyst (see text for more explanations).

impact on the selectivity in thiophene HDS. On the other hand, all the existing theory models converge on the conclusion that treatment with H_2S should favour increase of sulfur coverage of both Mo-edges and S-edges, whereas low chemical potentials of sulfur (treatment with H_2) should favour partially uncovered Mo-edges. If this was the cause of the observed effects, then a strong difference of catalytic properties between SS-400 and SH-400 would be further accentuated for higher treatment temperatures. In the experiment we observe quite an opposite trend. Therefore, the existing models need to be modified in order to account for these observations.

A coherent picture is obtained in this work relating the catalytic activity to the presence of extra-stoichiometric sulfur. The sulfhydryl groups are apparently in a dynamic equilibrium with S_2^{2-} edge moieties at each instant, but are progressively removed from the surface by hydrogen. It follows directly from the reaction mechanism (Scheme 1) that the HYD pathway should be more demanding for the –SH species than DDS pathway. That is why the samples containing more extra sulfur and therefore more of hydrogenating –SH groups are highly hydrogenating. Then, whatever the reason in the extra sulfur removal (reduction by hydrogen, or high-temperature thermal extrusion), the result is the same decrease of HDS activity and HYD selectivity.

Recently, Polyakov et al. showed that over-stoichiometric MoS_2 with S/Mo ratio >2 contains surface hydrogen, able to hydrogenate ethylene non-catalytically [26,27]. It might be questioned whether in the present work the same type of irreversible hydrogenation occurs, causing the effects observed. However, integration of the conversion curves during the first 24 h of reaction shows that the excess of butane produced by the S-saturated catalysts over that produced by the H-saturated samples was several times higher than the total molar amount of the catalyst. Moreover this high butane/butenes ratio remained stable at the experimental time scale and showed no trend to decrease during several days of further measurement on stream. Therefore, the hydrogen-containing species produced from the over stoichiometric sulfur are not irreversible hydrogen donors but represent true catalytic centres.

For a long time and until quite recently the field of HDS by sulfides was dominated by the concept of coordination unsaturated sites (CUS) as a principal constituent of active centres [57–60]. In these models CUS were considered essentially as the species obtained by the withdrawal of sulfur atoms from the regular stoichiometric MoS_2 edges. At the same time, several works indicated that over-stoichiometric sulfur may play a positive role for the catalytic activity, and the CUS formation is not the only condition for a good HDS performance. Several findings are difficult to explain on the base of CUS models, such as for instance, the well known fact that H_2S is a strong inhibitor for sulfur removal via the DDS route, but has only a minor effect on hydrogenation [61]. Earlier, a mechanism of thiophene adsorption was proposed without formation of CUS but rearrangement of S–S bonds [62]. More recently, on the base of STM measurements [63] and DFT calculations [64] it was suggested that fully sulfided Mo-edges might provide hydrogenation sites (brim sites). Moreover, according to DFT calculations the sulfur atoms should be stabilized as dimers on the fully sulfided MoS_2 edges, whereas H_2 molecules can be easily activated on S-dimer species [46]. Vogelaar et al. observed that the deactivation of a MoS_2/Al_2O_3 and a $NiMoS/Al_2O_3$ catalyst during the HDS of thiophene was due to the loss of sulfur from the active phase, while the extent of sintering/segregation and pore blocking had no significant effect on the activity [65]. Exposure to H_2S resulted in a partial reactivation, whereas exposure to H_2 led to deactivation. Farag et al. demonstrated that the activity for dibenzothiophene HDS over nanosized MoS_2 was strongly enhanced in the presence of H_2S. It was suggested that H_2S interacts with potential active sites resulting in new sites that showed a distinct activity [15]. From the insights of the present work, these findings receive a natural explanation. It should be emphasized, however, that our conclusions do not seem to extend beyond the reactions of sulfur-containing molecules. Indeed, for hydrogenation of molecules not containing sulfur, such as isoprene, the necessity of CUS presence at the MoS_2 edges has been well established [66].

3.2. Promoted catalysts

Nickel and cobalt were introduced by reflux with the respective acetylacetonates. This promotion technique recently developed by Bezverkhyy et al. [32], allows tailor-made synthesis of model HDS catalysts. The interaction with promoter occurs at 60 °C in methanol solution, being non-destroying for the MoS_2 fringes. According to characterization, neither the length of the slabs nor their stacking was changed after promotion. With some respect this method has common features with the CVD promotion technique developed by Okamoto and Kubota [67] or with impregnation using non-aqueous solutions as reported by Ji et al. [68]. In all cases the group 6 metal is sulfided before the interaction with promoter, being then put into contact with volatile carbonyl nitrosyl, or non–aqueous solution of nitrate or acetylacetonate.

The results of catalytic tests and the data of chemical analyses revealed a drastic difference between the catalysts obtained from the differently treated MoS_2, as exemplified in Fig. 12 for SS-400 and SH-400 (for other samples see Table 1). No promotion at all was obtained for the S-saturated systems. After reflux, low amounts of Ni or Co were found in these solids. TEM measurements showed that Co and Ni were not homogeneously distributed over the solids, but formed a few large particles of the corresponding sulfides Co_9S_8 and NiS (not shown). At the same time the amounts of Ni and Co spread over the MoS_2 particles, as detected by EDS, were lower than 1% at. Therefore, during the reflux Ni and Co complexes were rather occluded within the pores of MoS_2 or adsorbed on its basal planes, to form bulk-like particles upon further sulfidation. Worth noting is that the amorphous sulfide MoS_3 with its abundant S_2^{2-} structural units also showed a quite low promotion effect. A somewhat higher amount of cobalt retained by MoS_3 than by sulfur-saturated MoS_2 samples might be explained by the very high surface area of sponge-like MoS_3, which was able to occlude greater amounts of Co(AcAc).

High levels of promotion with Co and Ni were observed for the solids, treated at 400 °C in H_2. The amounts of metals accommodated on these solids were several times higher than for S-saturated ones and were comparable to the amount of hydrogen reversibly adsorbed on these samples, determined from the TPD

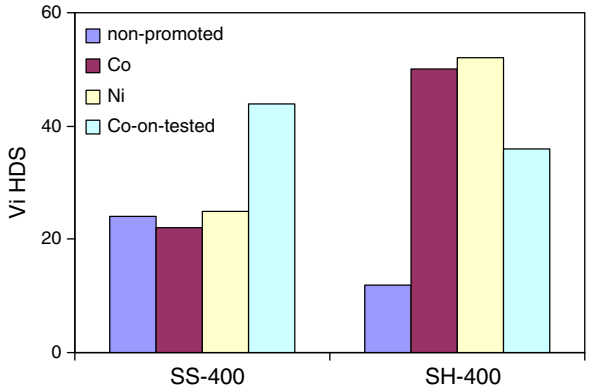

Fig. 12. Steady state thiophene HDS rates for the promoted and non-promoted catalysts SS-400 and SH-400. The "Co-on-tested" bars correspond to the catalysts obtained from the promotion of MoS_2 samples arrested after 16 h on stream thiophene test.

Scheme 2.

experiments. Similar promotion levels were observed for Ni and Co whatever the MoS_2 sample was. With the increase of the treatment temperature, a drop of the promotion level was observed for both H_2S- and H_2-treated sulfides. The results of thiophene HDS measurements on the promoted catalysts suggest that the S_2^{2-} moieties do not interact with Co(II) or Ni(II) ions from the solution, but that the –SH groups obtained after treatments with H_2 are able to exchange protons with the metals ions (Scheme 2). This is in agreement with an earlier reported method of titration –SH groups on the MoS_2 edges using their interaction with Ag^+ ions in solution [23].

To check whether our conclusions on the promoted and on the non-promoted solids were coherent, we tried to introduce cobalt in the MoS_2 catalysts taken after the HDS test (Fig. 12, "Co-on-tested" bars). In this case, the sulfur-saturated solid showed better promotion level, in accordance with expected formation of SH groups on its surface. For the H_2-treated SH-400 the promotion level after test was lower than for the fresh solid, probably due to the impurities and secondary reaction products (carbonaceous deposits, cf. Table 2) polluting the edges of MoS_2. Only the catalysts treated after 16 h on stream showed good promotion levels, whereas after 80 h of HDS the promotion effect was low.

The conclusions on the observed trends of promotion with Co(Ni) are possibly less general than for the non-promoted catalysts, since they might appear to be preparation-dependent. Therefore, further studies using alternative precursors (e.g. cobalt carbonyl nitrosyl) are planned to confirm or dismiss the generality of these conclusions. However, our preliminary studies show that in the case of promotion with Co and Ni nitrates dissolved in acetone, the promotion trends remain similar to those described above.

4. Conclusions

The principal result of this work is an insight into the role of over-stoichiometric sulfur, present in the unsupported sulfide catalysts in the form of surface S_2^{2-} species. The –SH groups produced from the S_2^{2-} groups by interaction with hydrogen seem to have a strong impact on the catalytic function of the MoS_2-based catalysts. It was shown that hydrogen-containing species formed from the over-stoichiometric sulfur participate in the catalytic reaction of thiophene conversion directly to butane (HYD pathway). Such hydrogenating centres are obviously distinct from coordinatively unsaturated sites (CUS), since they operate above the stoichiometry of MoS_2. When the extra sulfur is removed, the HYD function is suppressed. Unsupported MoS_2, if treated above 500 °C either in pure H_2 or in pure H_2S, becomes weakly hydrogenating. Further increase of temperature to 700 °C completely levels off the differences between the catalysts heated in pure H_2 and in pure H_2S (or in nitrogen). These observations have no straightforward explanation within the framework of current theories. The degree of stacking of MoS_2 slabs seems to have a less important role for thiophene HDS selectivity, since catalysts with similar morphology but strikingly different HYD/DDS selectivity were obtained, and also catalysts with similar selectivity but unequal stacking parameters.

Promotion seems to occur due to the interaction of Co(Ni) ions from the solution with the –SH groups located at the edges of the MoS_2 fringes. The affinity of nickel and cobalt ions toward the MoS_2 edges covered with S_2^{2-} species seems to be low. When the treatment temperature is increased, the promotion level decreases, whatever the gas atmosphere used (pure H_2S, H_2 or N_2). There is no significant difference between the promotion behaviour of Ni and Co for the preparation technique studied here. The findings reported in this work should be relevant for the interpretation of the TMS catalytic behaviour in both unsupported and supported catalysts.

Acknowledgment

The author thanks Pierre Delichere for technical assistance with XPS measurements.

References

[1] R.R. Chianelli, Catal. Rev. – Sci. Eng. 26 (1984) 361.
[2] H. Topsoe, B.S. Clausen, F.E. Massoth, Hydrotreating Catalysis, Science and Technology, Springer-Verlag, Berlin, 1996.
[3] S. Brunet, D. Mey, G. Perot, C. Bouchy, F. Diehl, Appl. Catal. A 278 (2005) 143.
[4] H. Topsøe, B.S. Clausen, R. Candia, C. Wivel, S. Morup, J. Catal. 68 (1981) 433.
[5] C. Wivel, R. Candia, B.S. Clausen, S. Morup, H. Topsøe, J. Catal. 68 (1981) 453.
[6] J.V. Lauritsen, S. Helveg, E. Lægsgaard, I. Stensgaard, B.S. Clausen, H. Topsøe, F. Besenbacher, J. Catal. 197 (2001) 1.
[7] F. Besenbacher, M. Brorson, B.S. Clausen, S. Helveg, B. Hinnemann, J. Kibsgaard, J.V. Lauritsen, P.G. Moses, J.K. Nørskov, H. Topsøe, Catal. Today 130 (2008) 86.
[8] P. Raybaud, J. Hafner, G. Kresse, H. Toulhoat, Surf. Sci. 407 (1998) 237.
[9] S. Cristol, J.-F. Paul, E. Payen, D. Bougeard, S. Clémendot, F. Hutschka, J. Phys. Chem. B 106 (2002) 5659.
[10] J.-F. Paul, S. Cristol, E. Payen, Catal. Today 130 (2008) 139.
[11] Y. Okamoto, A. Maezawa, T. Imanaka, J. Catal. 120 (1989) 29.
[12] L.S. Byskov, J.K. Norskov, B.S. Clausen, H. Topsoe, J. Catal. 187 (1999) 109.
[13] P. Raybaud, J. Hafner, G. Kresse, S. Kasztelan, H. Toulhoat, J. Catal. 189 (2000) 129.
[14] M. Daage, R.R. Chianelli, J. Catal. 149 (1994) 414.
[15] H. Farag, K. Sakanishi, M. Kouzu, A. Matsumura, Y. Sugimoto, I. Saito, J. Mol. Catal. A: Chem. 206 (2003) 399.
[16] L. Vradman, M.V. Landau, Catal. Lett. 77 (2001) 47.
[17] M. Li, H. Li, F. Jiang, Y. Chu, H. Nie, Fuel 88 (2009) 1281.
[18] V.M. Kogan, G.V. Isaguliants, Catal. Today 130 (2008) 243.
[19] J.T. Miller, W.J. Reagan, J.A. Kaduk, C.L. Marshall, A.J. Kropf, J. Catal. 193 (2000) 123.
[20] K. Inamura, R. Prins, Stud. Surf. Sci. Catal. 92 (1995) 412.
[21] E. Payen, S. Kasztelan, J. Grimblot, J. Mol. Struct. 174 (1988) 71.
[22] J. Polz, H. Zeilinger, B. Müller, H. Knözinger, J. Catal. 120 (1989) 22.
[23] J. Maternova, Appl. Catal. 3 (1982) 3.
[24] M. Lacroix, H. Jobic, C. Dumonteil, P. Afanasiev, M. Breysse, S. Kasztelan, Stud. Surf. Sci. Catal. 101 (1996) 117.
[25] H. Topsøe, B.S. Clausen, N.-Y. Topsøe, J.K. Nørskov, C.V. Ovesen, C.J.H. Jacobsen, Bull. Soc. Chim. Belg. 104 (1995) 283.
[26] M. Polyakov, M.W.E. van den Berg, T. Hanft, M. Poisot, W. Bensch, M. Muhler, W. Grünert, J. Catal. 256 (2008) 126.
[27] M. Polyakov, M. Poisot, W. Bensch, M. Muhler, W. Grünert, J. Catal. 256 (2008) 137.
[28] H. Farag, K. Sakanishi, M. Kouzu, A. Matsumura, Y. Sugimoto, I. Saito, Catal. Commun. 4 (2003) 321.
[29] J.C. Duchet, E.M. van Oers, V.H.J. de Beer, R. Prins, J. Catal. 80 (1983) 386.
[30] C. Loussot, P. Afanasiev, M. Vrinat, H. Jobic, P.C. Leverd, Chem. Mater. 18 (2006) 5659.
[31] P. Afanasiev, H. Jobic, C. Lorentz, P. Leverd, N. Mastubayashi, L. Piccolo, M. Vrinat, J. Phys. Chem. C 113 (2009) 4139.
[32] I. Bezverkhyy, P. Afanasiev, M. Lacroix, J. Catal. 230 (2005) 133.
[33] D.G. Kalthod, S.W. Weller, J. Catal. 95 (1985) 455.
[34] H. Nava, F. Pedraza, G. Alonso, Catal. Lett. 99 (2005) 65.
[35] Y. Yoneyama, C.S. Song, Catal. Today 50 (1999) 19.
[36] J.L. Brito, M. Ilija, P. Hernández, Thermochim. Acta 256 (1995) 325.
[37] D. Genuit, P. Afanasiev, M. Vrinat, J. Catal. 235 (2005) 302.
[38] Y. Iwata, Y. Araki, K. Honna, Y. Miki, K. Sato, H. Shimada, Catal. Today 65 (2001) 335.
[39] C. Calais, N. Matsubayashi, C. Geantet, Y. Yoshimura, H. Shimada, A. Nishijima, M. Lacroix, M. Breysse, J. Catal. 174 (1998) 130.
[40] F. Labruyère, M. Lacroix, D. Schweich, M. Breysse, J. Catal. 167 (1997) 464.
[41] D. Gulková, Y. Yoshimura, Z. Vít, Appl. Catal. B 87 (2009) 171.
[42] T. Komatsu, W.K. Hall, J. Phys. Chem. 95 (1991) 9966.
[43] L. Jalowiecki, A. Aboulaz, S. Kasztelan, J. Grimblot, J.P. Bonnelle, J. Catal. 120 (1989) 10.
[44] X.S. Li, Q. Xin, X.X. Guo, P. Grange, B. Delmon, J. Catal. 137 (1992) 385.
[45] M. Breysse, E. Furimsky, S. Kasztelan, M. Lacroix, G. Perot, Catal. Rev. Sci. Eng. 44 (2002) 651.
[46] M. Sun, A.E. Nelson, J. Adjaye, Catal. Today 105 (2005) 36.
[47] C.H. Chang, S.S. Chan, J. Catal. 72 (1981) 139.

[48] G.L. Schrader, C.P. Cheng, J. Catal. 85 (1984) 488.
[49] G.L. Frey, R. Tenne, Phys. Rev. B 60 (1999) 2883.
[50] M.A. Baker, R. Gilmore, C. Lenardi, W. Gissler, Appl. Surf. Sci. 150 (1999) 255.
[51] J.C. Muijsers, Th. Weber, R.M. van Hardeveld, H.W. Zandbergen, J.W. Niemantsverdriet, J. Catal. 157 (1995) 698.
[52] S.J. Hibble, M.R. Feaviour, J. Mater. Chem. 11 (2001) 2607.
[53] S.J. Gregg, K.S.W. Sing, Adsorption Surface Area and Porosity, Academic Press, London, 1991.
[54] D.L. Sullivan, J.G. Ekerdt, J. Catal. 178 (1998) 226.
[55] M.L. Vrinat, Appl. Catal. 6 (1983) 137.
[56] P. Tétényi, V. Galsàn, React. Kinet. Catal. Lett. 78 (2003) 299.
[57] F.E. Massoth, J. Catal. 36 (1985) 164.
[58] C. Vogdt, T. Butz, A. Lerf, H. Knozinger, Polyhedron 5 (1986) 95.
[59] C.J.H. Jacobsen, E. Tornqvist, H. Topsøe, Catal. Lett. 63 (1999) 179.
[60] F. Dumeignil, J.F. Paul, E. Veilly, E.W. Qian, A. Ishihara, E. Payen, T. Kabe, Appl. Catal. A 289 (2005) 51.
[61] M. Egorova, R. Prins, J. Catal. 225 (2004) 417.
[62] T.S. Smit, K.H. Johnson, J. Mol. Catal. 91 (1994) 207.
[63] J.V. Lauritsen, M. Nyberg, J.K. Nørskov, B.S. Clausen, H. Topsøe, E. Lægsgaard, F. Besenbacher, J. Catal. 224 (2004) 94.
[64] P.G. Moses, B. Hinnemann, H. Topsøe, J.K. Nørskov, J. Catal. 248 (2007) 188.
[65] B.M. Vogelaar, P. Steiner, Th.F. van der Zijden, A.D. van Langeveld, S. Eijsbouts, J.A. Moulijn, Appl. Catal. A 318 (2007) 28.
[66] A. Wambeke, L. Jalowiecki, S. Kasztelan, J.P. Grimblot, J.P. Bonnelle, J. Catal. 109 (1988) 320.
[67] Y. Okamoto, T. Kubota, Catal. Today 86 (2003) 31.
[68] Y. Ji, P. Afanasiev, M. Vrinat, W. Li, C. Li, Appl. Catal. 257 (2004) 157.